Journal of Cluster Science
https://doi.org/10.1007/s10876-024-02699-6

ORIGINAL PAPER

Simultaneous Delivery of Dual Anticancer Agents Via pH-Responsive Polymeric Nanoparticles for Enhanced Therapeutic Efficacy Against Breast Cancer Cells

Muhammad Haroon[1] · Mehwish Nasim[1] · Asif Nawaz[1,8] · Naveed Ullah Khan[2] · Sheikh Abdur Rashid[1] · Daulat Haleem Khan[3] · Muhammad Khurshid Alam Shah[1] · Mohammad Y. Alfaifi[4,5] · Serag Eldin I. Elbehairi[4,5] · Ali A. Shati[4,5] · Haroon Iqbal[6,7]

Received: 7 May 2024 / Accepted: 7 September 2024

Abstract
The stated objective of the present research investigation was to use a simultaneous nanodrug delivery approach to optimize the therapeutic effectiveness of anticancer drugs against breast cancer cells. For this purpose, Poly (lactic-co-glycolic acid) nanoparticles with two anticancer drugs; methotrexate (MTX) and doxorubicin (DOX) denoted as DOX/MTX@PLGA NPs was developed by nanoprecipitation method. The developed polymeric DOX/MTX@PLGA NPs exhibited hydrodynamic particle diameter of 170.6 ± 10.0 nm with a poly dispersity index (PDI) of 0.17 and zeta potential value of -9.2 ± 0.31 mV, and spherical geometry analyzed by TEM. Furthermore, the nanoparticles exhibited a pH-responsive drug release profile, outstanding encapsulation efficiency, excellent colloidal stability across various physiological media and pH responsive drug release profile. Additionally, polymeric nanoparticles demonstrated higher cell uptake, in-vitro cytotoxicity, and a high rate of apoptosis in comparison to free DOX and MTX through a synergistic effect, likely as a result of their small particle size. In conclusion, our work presents a novel and distinct approach for boosting the therapeutic efficacy of anticancer drugs by delivering drugs to breast cancer cells simultaneously.

Keywords Doxorubicin · Breast cancer · Nanoprecipitation · Cell Uptake · In-vitro drug release · Cell apoptosis

Introduction

Cancer is the second most common cause of death and morbidity worldwide, with a high incidence rate [1]. The World Health Organization (WHO) declares the primary cause of cancer-related mortality for women is breast cancer, which accounts for up to 29% of all female malignancies worldwide [2, 3]. In addition to surgery, chemotherapy is still the primary cancer treatment option [4]. The first-line chemotherapy treatment approach for breast cancer involves the use

✉ Sheikh Abdur Rashid
sarashid@gu.edu.pk

✉ Haroon Iqbal
haroonigbal415@hotmail.com

1 Gomal Centre of Pharmaceutical Sciences, Faculty of Pharmacy, Gomal University, Dera Ismail Khan 29050, Pakistan

2 Department of Pharmacy, Zhejiang University of Technology, Hangzhou 310000, China

3 Lahore College of Pharmaceutical Sciences, Lahore 54000, Pakistan

4 Faculty of Science, Biology Department, King Khalid University, Abha 9004, Saudi Arabia

5 Tissue Culture and Cancer Biology Research Laboratory, King Khalid University, Abha 9004, Saudi Arabia

6 Hangzhou Institute of Medicine, Zhejiang Cancer Hospital, Chinese Academy of Sciences, Hangzhou, Zhejiang 310022, China

7 State Key Laboratory of Ophthalmology, Optometry and Visual Science, Eye Hospital, School of Ophthalmology and Optometry, Wenzhou Medical University, Wenzhou, Zhejiang 325027, China

8 Faculty of Pharmacy, Universiti Sultan Zainal Abidin, Besut Campus, Besut, Terengganu 22200, Malaysia

Published online: 21 September 2024

of anticancer drugs such as doxorubicin (DOX), docetaxel, and paclitaxel [5]. However, a number of challenges have the potential to render the administration of these chemotherapeutic agents difficult. These problems include poor aqueous solubility, quick elimination, non-specific distribution, which requires the administration of higher doses and leads to dose-related toxicities, and a lack of specificity to keep the anti-cancer drug in the cancerous region [6]. These reasons paved the way for major global research initiatives with the goal of developing a more effective cancer treatment approach [7].

Nanotechnology has become an essential tool in the field of biomedicine, helping to treat a wide range of ailments, notably cancer [8, 9]. Therefore, the utilization of nanosized formulations as delivery systems for a variety of medicinal compounds, including proteins, nucleotides, and diagnostic imaging agents, has been extensively employed [10, 11]. Several research investigations demonstrate that advancements in the administration of chemotherapeutic drugs via nanocarriers could result in more effective treatment for cancer. A variety of novel nanocarrier technologies have been developed by researchers to improve the delivery of anticancer drugs, especially to cancerous sites. For example, liposomes are biocompatible nanocarrier, and considered as a delivery system for encapsulating anti-cancer drugs [12]. However, there's a significant issue with insufficient stability, low drug release and storage [13]. The appropriate application of nanoparticles (NPs) in the administration of drugs is vital [14]. Polymeric NPs' strong framework and integrity enables controlled and sustained drug release [15]. Poly (lactic-co-glycolic acid) (PLGA), a copolymer of poly (lactic acid) and poly (glycolic acid), has been approved by the FDA for drug encapsulation. It is among the biomaterials with the most outstanding characteristics. Three things that contribute to this include its established controlled drugs release, being biodegradability and biocompatibility [16].

Doxorubicin (DOX) is an antineoplastic agent and belongs to non-selective class I anthracycline antibiotic group. It is one of the most effective available chemotherapeutic agent [17]. In medical procedures, it has been administered to treat different kinds of cancers either alone or in combination [18]. Irrespective of its potential benefits, DOX may result in dosage-dependent cardiac toxicities, including chronic cardiomyopathy and congestive heart failure [19]. Second, drugs efflux from cancerous cells may increase due to multidrug resistance (MDR), which might render cancer treatment inefficient [20]. It has been widely recognized that NPs-based drug delivery approaches, which include NPs, offer advantages over free drugs [21], liposomes [22] and cyclodextrins [23], exhibit auspicious anticancer features due to their increased bioavailability and less adverse effects [24].

Methotrexate (MTX) inhibit the dihydrofolate reductase enzyme activity and shows antitumor activity. MTX, which is ranked 20th on the World Health Organization's Model List of Essential Medicines, is considered an essential drug by oncologists [25].

Since MTX is not the first-line therapy for breast carcinoma, lots of research are being conducted to increase its efficacy, some of which entail combining it with a variety of other anticancer drugs [26]. MTX is generally effective in treating breast cancer in women, including metastatic cancer and patients in which radiation and surgery have already been performed.

It has been established that multidrug resistance (MDR) in breast cancer cells is one of the biggest challenges associated with breast cancer therapy. It has been found that MCF-7 breast cancer cell lines are resistant to cytotoxic agents such as DOX for several reasons. It has been discovered that NPs-based combination treatments are useful in treating MDR. Thus, a study was carried out to examine how MTX and DOX interact with MCF-7 cells. To our knowledge, this is the first time that MTX and DOX are being evaluated simultaneously against MCF-7 cells. Treating resistant breast cancer more effectively could be aided by this combinatorial method.

In a nutshell, the current effort aimed to design and optimize DOX/MTX@PLGA NPs for combination therapy by means of a trial-and-error methodology that would make it possible for controlled simultaneous release of anti-cancer drugs. PLGA was utilized as an outer shell because of its biodegradability and biocompatibility. PLGA shell protect drugs from degradation and facilitate absorptive transcytosis into the endothelium cortex [27]. PLGA NPs loaded with two anticancer drugs were developed by a single-step modified nanoprecipitation method [28]. Apart from executing diverse physio-chemical characterization assessments, the release patterns of DOX/MTX@PLGA NPs and in-vitro tests conducted on cancer cell lines were also assessed.

Our study's results provide credence to the idea that polymeric NPs enhance the therapeutic efficacy of MTX and DOX, present an attractive choice for the management of breast cancer, and pave the way for additional research investigations. In conclusion, this work opens up prospective possibilities for research into encapsulating DOX and MTX in PLGA NPs for breast cancer treatment.

Materials and Methods

Materials

Methotrexate (MTX) and Doxorubicin (DOX) were procured from Tokyo Chemical Industry Co. Ltd, Japan,

Sodium phosphate dibasic (Na_2HPO_4) and Dimethylformamide (DMF) were procured from Sigma Aldrich, chemical company. St. Louis, MO, USA. Triton X-100, Dimethyl sulfoxide (DMSO), Dulbecco's Modified Eagle Medium (DMEM), phosphate buffered saline (PBS), Hank's balance salt solution (HBSS), fetal bovine serum (FBS, 10%), trypsin (2.5%), Poly (D, L-lactide-co-glycolide) (PLGA, 50:50; molecular weight: 30,000–60,000), Polyvinyl alcohol (PVA), non-essential amino acids (NEAA) and penicillin-streptomycin (PEST) were purchased from Sigma Aldrich, Germany). MCF-7, a human breast cancer cell line (ATCC, Manassas, VA). The buffer was prepared and formulated using Milli-Q water (Merck Millipore, USA). Furthermore, HPLC-grade solvents and other analytically-grade chemicals along with reagents were used in the investigation.

Preparation of DOX/MTX@PLGA NPS

Slight adjustments were made to the single-step nanoprecipitation process to fabricate the self-assembled blank and drug-loaded PLGA NPs [29]. MTX (5 mg) and PLGA (2 mg/ml) were dissolved in dimethylformamide (DMF) for preparing the organic phase of the reaction. 10 mg of the DOX was dissolved in PLGA solution. The PVA solution (0.5–1.0%) made up the aqueous phase. Through constant stirring and the use of a syringe pump with a constant flow rate of 1 mL/min, the organic phase was gradually added to the water phase.

NPs were allowed to self-assemble by agitating the already-prepared solution for 2 h at a steady temperature of 30 °C at an average speed of 600 rpm.

Eventually, the synthesized nanoparticles endured three rounds of centrifugation and Milli-Q water washing with an Amicon ultracentrifugation filter (10 kDa). A univariate, one variable at a time technique was used for obtaining the optimal formulation (data not shown).

After being suspended in sucrose solution (2% w/v), the nanoparticles were lyophilized (LyoQuest, Telstar, Shanghai, China) and stored at 4 °C for further research investigations.

Physio-Chemical Characterization of DOX/MTX@PLGA NPs

Particle Size, PDI and Surface Charge Analysis

With the use of an analyzer (Malvern Instruments, UK), the synthesized DOX/MTX@PLGA NPs' average particle size, hydrodynamic diameter, and distribution (PDI) in an aqueous solution at a 90° scattering angle and optimum time of 60 s between cycles were measured. The nanoparticles enclosing cell was exposed to voltage across both electrodes in order to determine the zeta potential of DOX/MTX@PLGA NPs. Each of the samples was evaluated separately three times [30].

Surface Morphology

The morphological properties of DOX/MTX@PLGA NPs were investigated utilizing TEM (Jeol JEM-1400, Jeol Ltd, Tokyo, Japan). 5 µL of the diluted dispersion was applied to a copper grid, which was then dried at room temperature and photographed using a TEM after being negatively stained for 2 min with 2% v/v uranyl acetate [31].

Encapsulation Efficiency and Drug Loading

To calculate the percentage drug loading (DL%) and the percentage of effective encapsulation (EE%) of the DOX/MTX@PLGA NPs, the drugs were recovered from the nanoparticles using methanol. The extracted drug samples were then analyzed using a UV spectrophotometer (Shimadzu UV-1800, Kyoto, Japan) at a wavelength of 480 nm and 302 nm for DOX and MTX, respectively. The relevant standard curve was then used to calculate the recommended amount of the drug [32].

FTIR Analysis

The generated nanoparticles were subjected to FTIR spectroscopy (Bruker, Karlsruhe, Germany) For the purpose of confirming the existence of relevant functional groups and any intramolecular interactions among the drugs and PLGA, the synthesized Nanoparticles were investigated using FTIR spectroscopy studies [33]. In short, incredibly small quantities of freeze-dried powders of free DOX, free MTX, blank NPs, and DOX/MTX@PLGA NPs were introduced into the sample chamber instantaneously. The infrared spectrum was subsequently determined for 120 scans over a range of 500–4000 cm^{-1} at a resolution of 4 cm^{-1} and a scanning speed of 2 mm sec^{-1}.

Differential Scanning Calorimetry (DSC)

The DSC spectra of blank NPs, free MTX, free DOX, and DOX/MTX@PLGA NPs were recorded using a concurrent thermal analyzer (DSC 823e, Mettler Toledo, USA). A sealed aluminum pan was used to heat every single freeze-dried sample to a temperature of 250 °C at a rate of 10 °C per minute while maintaining an uninterrupted nitrogen flow of 30 mL min^{-1}. As a reference check, a tightly sealed blank aluminum pan has been used [34].

Powder X-ray Diffraction Analysis (pXRD)

The X-ray spectra of free DOX, free MTX, blank NPs, and DOX/MTX@PLGA NPs were recorded using an X-ray diffractometer (Almelo, Netherlands) that was set to operate at a specified wavelength of 1.5406Å, scan step size of 0.02°, scan step time of 17.7 s, voltage of 40 kV, and current of 40mA [35].

In-vitro Drug Release

The membrane-mediated dialysis technique was used to calculate the in-vitro drug release from DOX/MTX@PLGA NPs with the objective to mimic the drug delivery system's ultimate effectiveness within biological fluids. In the aforementioned approach, 1 mL of the NPs suspension was incorporated, with respect to the DOX concentration of 150 µg/mL and the MTX concentration of 220 µg/ml, using dialysis bags (Solarbio, Beijing, China) with an average cutoff molecular weight of 8–14 kDa. A 15 mL centrifuged tube containing 10 ml of PEG 400 (30% v/v) dissolution medium was filled with clip-sealed dialysis bags so that the release of the DOX and MTX could be monitored throughout a period of 48 h. At a controlled temperature of 37 ± 1 °C, the tubes were subjected to shaking at 150 rpm per min.

Finally, at predetermined intervals of time, particularly 0, 0.5, 1, 2, 4, 6, 8, 12, 18, 24 and 48 h, 200 µL of the specimen was drawn out in triplicate. To keep the volume constant for the entire period of the course of the investigation, the dissolving medium was refilled with an equivalent volume of fresh solution media at the same temperature in order to maintain the sink condition.

A UV spectrophotometric analysis (Shimadzu UV-1800, Kyoto, Japan) was performed to determine the total amount of MTX and DOX released from DOX/MTX@PLGA NPs at 480 nm and 302 nm, separately [36].

Colloidal Stability Determination

The long-term stability of the prepared DOX/MTX@PLGA NPs in various physiological mediums (PBS, DMEM, 8% glucose, 0.9% NaCl, and distilled water) was evaluated using the previously described method in order to assess the possible in-vivo behavior [29]. Briefly stated, 0.1 mg of freeze-dried DOX/MTX@PLGA NPs were added to 1 mL of each solution, and the mixture was constantly agitated at 100 rpm and 37 °C. Following three experimental repetitions and graphical data presentation, 200 µL of each sample solution were extracted at predetermined intervals and subjected to the Zeta sizer for evaluation of PDI, mean particle size, and zeta potential.

Cell Studies

Cell Lines

MCF-7 cells were cultured in DMEM culture medium in a gas incubator (BB 16 gas incubator, Heraeus Instruments GmbH) with the following parameters: 37 °C, 95% humidity, and 5% CO2. As additions to the cell culture medium, 1% PEST, 1% NEAA, and 10% FBS were added. Before every test, the cells were defrosted, sub cultured at 80% convergence, and seeded for additional experiments.

Cell Uptake Analysis

To conduct an analysis of DOX/MTX@PLGA NPS cell uptake in MCF-7 cells, minor adjustments have been made to a previous research methodology [29]. In short, 4×10^5 MCF-7 cells were introduced into each well of 24 well plates containing 0.5 mL RPMI-1640 with FBS (10%) and allowed to remain attached to the culture plate for a whole day. To ascertain the time-dependent cellular absorption of drugs in PLGA nanoparticles, cells were incubated for several time intervals (4, 6, 12, and 24 h) with DOX/MTX@PLGA NPs (2.5 µg/ml). Untreated cells were present in the control group. To separate the cells from the plates, wells were treated with 0.1% Triton X-100 after being twice-washed with PBS (pH 7.4). The integrated drugs were then completely dissolved by injecting ACN: H_2O (6:4). The obtained cell lysate was spun at 25,000 rpm for 15 min.

Utilizing methanol as a solvent and a UV spectrophotometer (Shimadzu UV-1800, Kyoto, Japan) calibrated to measure at 480 nm and 302 nm, respectively, using standard calibrated curves for DOX and MTX, the quantity of integrated drugs was then calculated. A triplicate reading was taken, and the mean ± SD was displayed as the outcome of the experiment.

Mechanism of Cell Uptake

To study the cellular absorption processes or endocytic system of DOX/MTX@PLGA NPs, MCF-7 cells were cultured at a density of 1×10^5 in wells packed with medium of RPMI-1640 (1 mL) and FBS (10%) for 24 h.

The cells were supplied with fresh medium, aspirated, and cold washed with phosphate buffer solution once they had grown. In accordance with earlier research, the cells were pre-incubated with additional inhibitors in the subsequent phase at non-detrimental doses [37]: To prevent clathrin-mediated endocytosis, use a concentration of 10 µg/mL of chlorpromazine (Sigma-Aldrich); to inhibit caveolae-mediated endocytosis, use a concentration of 2 µg/mL of nystatin (Sigma-Aldrich); and to inhibit macro-pinocytosis,

use a concentration of 100 µg/ml of amiloride (Sigma-Aldrich). MCF-7 cells were cultured at 4 °C for a period of 12 h with the intention to evaluate the active and passive transport pathways.

The inhibitor solutions were withdrawn and freshly synthesized nanoparticles were introduced to the inhibitor containing medium at the same doses after a 24 h pre-incubation period at 37 °C. There was an instantaneous 2 h incubation period after this. As was previously described, the cells were washed. The control group was given DOX/MTX@PLGA NPs and had 100% uptake even though they failed to receive inhibitor drugs.

Intracellular Distribution

In MCF breast cancer cells, the intracellular distribution of DOX/MTX@PLGA NPs was observed using confocal microscopy. In this instance, MCF-7 cells were seeded at a density of 5×10^4 into a glass-bottomed confocal imaging dish containing 1.5 mL RPMI-1640 with FBS (10%). For twelve hours, the cells were cultured under 5% CO2. The cells were then incubated for an additional 4 h at 37 ºC after being treated with DOX/MTX@PLGA NPs, free DOX, and free MTX (10 µg/ml for each). Following process completion, the medium was aspirated, the cells were rinsed three times with phosphate buffer solution, and they subsequently stained for five min with 5 µg/ml of Hoechst.

The cells were stained for an additional ten minutes using lysotracker green dye after being meticulously cleaned five more times with PBS. Employing confocal laser scanning microscopy (CLSM 510 META), the cells were analyzed after being rinsed five times with PBS in the last stage [29].

Cell Viability Analysis

The MTT test was used for determining the cytotoxicity of DOX/MTX@PLGA NPs on the viability of MCF-7 cells. MCF-7 cells were cultivated in 96-well plates at a density of 2×10^4 cells per well for 24 h following reported protocol with minor modifications [38].

At various doses, DOX/MTX@PLGA NPs were used for the treatment of the cells. Following a 24 h incubation period, 100 µL of new media and 10 µL of MTT solution (5 mg/mL) were added to each well, and the plate was left for cell culture for an extra 4 h. After removing the previous growth media and unreduced MTT, 150 µL of DMSO was added to each well to dissolve the formazan crystals. Following a 10-second agitation period, and the absorbance which shows the direct estimation of living and dead cells was recorded at 492 nm using Spark multifunctional microplate reader (Hombrechtikon, Switzerland) [39].

In-vitro Cell Apoptosis

Flow cytometry was used to determine if DOX/MTX@PLGA NPs might trigger apoptosis in MCF-7 cells [40]. In short, 5×10^4 MCF-7 cells were injected into each well of twelve well culture plates 1.5 mL RPMI-1640 with FBS (10%), and the cells were allowed to develop for 12 h in an incubator with 5% CO2. The cells were then incubated for 12 h with an equal amount of free drugs (5 µg/ml) and DOX/MTX@PLGA NPs. According to the manufacturer's recommendations, the flow cytometer was used to measure the cell apoptosis after a 12-hour period using BD FACS Canto II, BD Biosciences, USA, and Annexin V-APC/DAPI Apoptosis Detection Kit I, BD Biosciences, USA [41].

Chou-Talalay Analysis

To investigate the potential synergistic effects of two drugs, PLGA NPs were applied to MCF-7 cells at various DOX-MTX weight ratios. Using Chou-Talalay methods of analysis, the dosage effect data relevant to drug doses and the fraction of afflicted tumor cells (Fa) were examined.

The data analysis program CompuSyn was used to calculate the combination index values. MCF-7 cells were treated for 48 h with a mixture of DOX and MTX in the form of free drugs and NPs with different modifications for a selected weight ratio [42].

Statistical Analysis

Every test was carried out in triplicate in a sequential manner to confirm the accuracy and reproducibility of the obtained results. All the data was presented as mean ± SD. The significance level was calculated using student's *t-tests* (OriginPro8 software, OriginLab Corporation, Northampton, MA, USA). The statistical analysis revealed that the results were significant for $p<0.05$ and insignificant for $p>0.05$, respectively.

Results and Discussion

Preparation and Characterization of Combined (DOX/MTX) PLGA NPs

Synergistic breast cancer chemotherapy was achieved by effectively fabricating PLGA NPs co-loaded with two anticancer drugs, DOX and MTX, by a one-step nanoprecipitation method. Based on TEM investigation, the synthesized DOX/MTX@PLGA NPS had a spherical and smooth shape, as Fig. 1A and B illustrate. Furthermore, based on DLS assessment, the average hydrodynamic particle size of

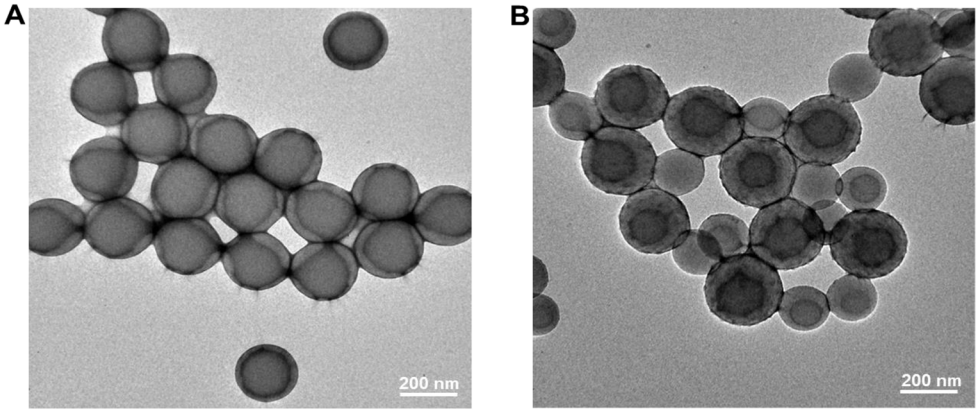

Fig. 1 Surface morphology analysis by TEM (**A**) Blank PLGA NPs. (**B**) DOX/MTX@ PLGA NPs

Table 1 Percentage of drug loading and encapsulation effectiveness of MTX and DOX in DOX/MTX@PLGA NPs

Formulation Code	DOX loading (%)	MTX loading (%)	DOX EE (%)	MTX EE (%)
DOX/MTX@PLGA NPs 1	2.67 ± 0.27	3.62 ± 0.52	78.68 ± 1.29	77.61 ± 2.59
DOX/MTX@PLGA NPs 2	3.56 ± 1.30	4.09 ± 0.11	79.93 ± 2.47	80.09 ± 1.40
DOX/MTX@PLGA NPs 3	4.17 ± 1.29	6.13 ± 0.56	81.72 ± 3.21	82.83 ± 2.69

DOX/MTX@PLGA NPs 3 represents optimized formulation; Data were expressed as mean ± SD ($n = 3$)

DOX/MTX@PLGA NPs was 170.6 ± 10.0 nm, exhibiting a narrow range of size (0.17), as shown in (Table 1).

The hydrodynamic particle diameters of DOX/MTX@ PLGA NPs were significantly larger than those of blank NPs (99.07 ± 5.2 nm). One possible explanation for this increase in size could be the loading of drugs into PLGA NPs. Formulations with lower particle sizes (less than 200 nm) demonstrated superior cellular penetration and absorption in comparison to formulations with larger particle sizes [43].

Given that DOX/MTX@PLGA NPs had an average particle size of less than 200 nm, there may be additional potential for improved cellular absorption. Furthermore, DOX/ MTX@PLGA NPs displayed a surface charge of -9.2 ± 0.31 mV, demonstrating adequate surface charges to prevent their accumulation in a physiological milieu [44]. The negative surface charges on DOX/MTX@PLGA NPs decreases compared to blank NPs (-24.3 ± 0.3 mV) after drug loading, indicating the successful encapsulation of drugs in PLGA NPs (Fig. 2C & D).

The effectiveness of loading and encapsulating DOX and MTX into hybrid PLGA NPs was ascertained through the use of UV spectroscopic examination. Table 1 shows that the DL of DOX/MTX@PLGA NPs was 4.17 ± 1.29% for DOX and 6.13 ± 0.56% for MTX. Similarly, the EE was found to be 81.72 ± 3.21% for DOX and 82.83 ± 2.69% for MTX.

The FTIR spectra of blank NPs, free DOX, free MTX, and DOX/MTX@PLGA NPs were displayed in Fig. 3A. FTIR spectrum of free DOX revealed characteristic bands at 3552, 3318, 2932, 1729, 1617, and 1579 cm^{-1}, respectively. These bands represent amide I and II groups bending vibrations overlapped with anthracene ring C = O, N-H asymmetric stretching, C-H stretching, and C-O stretching [45]. In the FTIR spectrum, the characteristic bands for MTX can be observed at 3359 cm-1 and 2937 cm^{-1}, which represent O-H stretching of COOH and N-H asymmetric stretching, correspondingly.

The distinct bands at 1640 cm^{-1} and 1522 cm^{-1}, which represent the bending of CN-H amide II and the C = O stretching of COOH, respectively, are caused by MTX [46]. The presence of the benzene ring and carboxylic acid's -O-H bending is indicated by the absorption bands at 979 cm^{-1} and 820 cm-1, respectively. These characteristic bands have been well-described in previous studies [47]. The FTIR spectra of the blank Nanoparticles revealed the hallmark bands of the PLGA at 1747 cm^{-1}, 1452 cm^{-1}, and 1332 cm^{-1}, which represent -C = O symmetric stretching, C-H bending, and so on. All of the distinctive peaks for DOX, MTX, and PLGA were visible in the FTIR spectra of freeze-dried DOX/MTX@PLGA NPs, with no discernible structural modifications during NP assembly. In addition, the development of NPs is demonstrated by the enlargement, alteration, or elimination of a few characteristic peaks.

In Fig. 3B, the X-ray diffractograms of blank, free drugs, and DOX/MTX@PLGA NPs were displayed. The most intense and sharp peaks at 10.2, 17.2, 22.3, 24.1, 27.9, and 33.3 for DOX and 10.8, 14.5, 17.5, 19.4, 22.5, and 37.5 for MTX (2θ) confirmed the crystalline nature of free drugs [48, 49]. However, no sharp and intense peak of DOX and MTX were observed in DOX/MTX@PLGA NPs diffractograms, indicating the conversion of crystalline DOX and MTX into amorphous state upon encapsulation in PLGA NPs. The solubility and bioavailability of both DOX and MTX may have been enhanced by this transformation, as amorphous

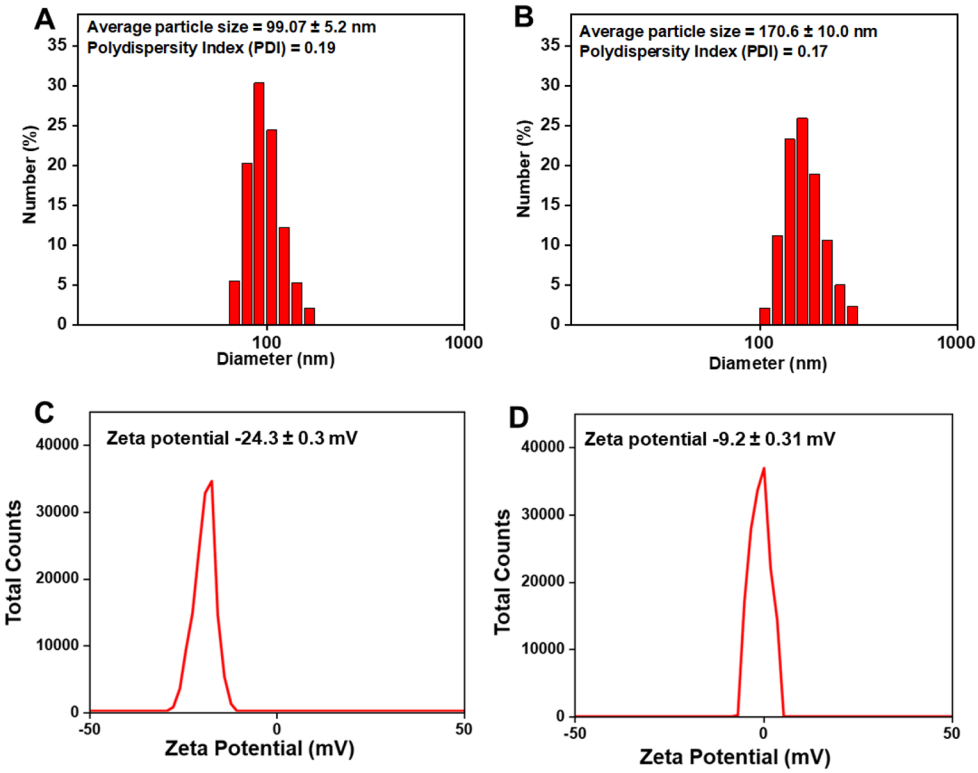

Fig. 2 Characterization of DOX/MTX@PLGA NPs. (**A**) Hydrodynamic diameter of blank PLGA NPs. (**B**) Hydrodynamic diameter of DOX/MTX@PLGA NPs. (**C**) Zeta potential of blank PLGA NPs. (**D**) Zeta potential of DOX/MTX@PLGA NPs

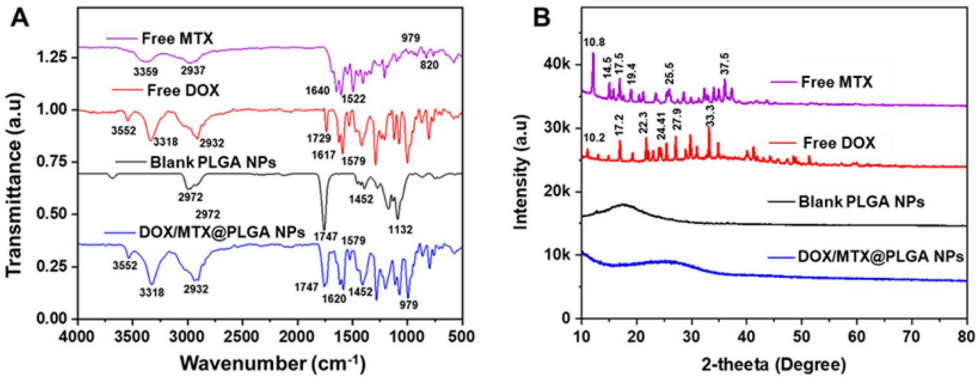

Fig. 3 (**A**) FTIR spectra of blank PLGA NPs, free DOX, free MTX, and DOX/MTX@PLGA NPs (**B**) X-ray diffractograms of blank PLGA NPs, free MTX, free DOX, and DOX/MTX@PLGA NPS

drugs exhibit higher solubility than crystalline ones. DSC thermograms of free drugs, blank NPs, and DOX-MTX-PLGA NPs are displayed in Fig. 4A. At 232 °C and 150 °C, respectively, DOX and MTX both showed their characteristic sharp peaks, indicating crystalline nature of free drugs DOX and MTX [50, 51]. However, neither drug's significant melting point peaks were seen in the thermograms of DOX/MTX@PLGA NPs, suggesting that the drug's amorphous form had established at the time of NPs encapsulation.

The formation of bigger agglomerates is a high-inclination characteristic of nanosized particles dispersed in physiological media, and dispersion stability is an important characteristic [52]. The average particle size was evaluated at specified times to evaluate the colloidal stability of DOX/MTX@PLGA NPs for 120 h (5 days) at 4 ºC in different physiological mediums (DMEM, 8% glucose, 0.9% NaCl, PBS, and distilled water). After incubating NPs with various physiological media at 4 ºC for 5 days, the particle size study's results showed no discernible change in the average particle size of the NPs (Fig. 4B). Strong repulsions between the NPs in the dispersion are caused by the PLGA surface charge, which could be the reason for the NPs' enhanced colloidal stability [28]. The strong repulsions keep the NPs from getting too near to one another. Therefore, aggregation would have to be rare in this kind of environment [53].

In-vitro Drug Release and Kinetic Modeling

At pH 5.0 and pH 7.4, which mimic the exact conditions that the NPs encountered upon entering the lysosomal compartment, the in-vitro drug release from DOX/MTX@PLGA

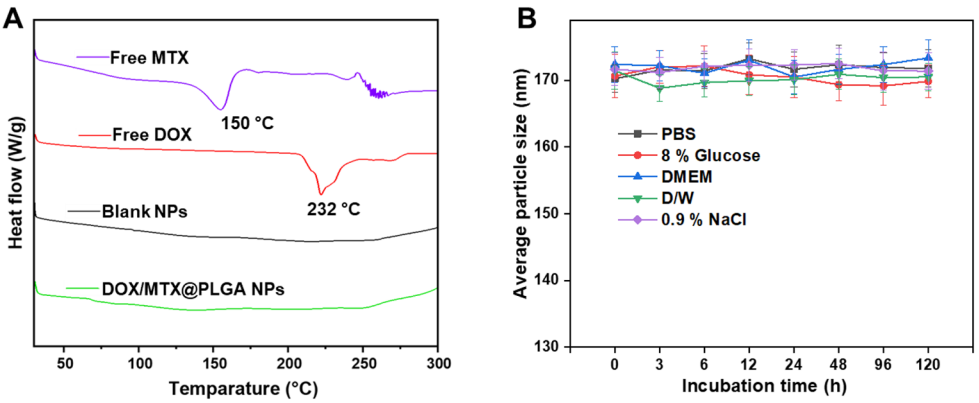

Fig. 4 (**A**) DSC thermograms of blank NPs, free MTX, free DOX, and DOX/MTX@PLGA NPs (**B**) DOX/MTX@PLGA NPs maintained their colloidal stability over 120 h in a variety of physiological media. (mean ± SD, $n = 3$)

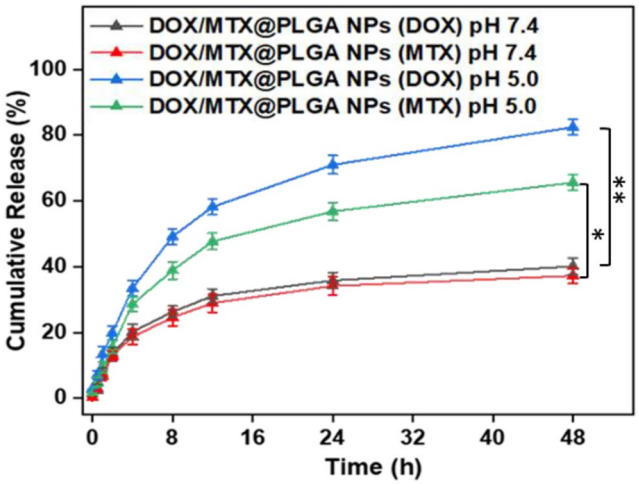

Fig. 5 In-vitro drug release profile of DOX and MTX from DOX/MTX@PLGA NPs at pH 5.0 and 7.4. Data are expressed as a mean ± SD, $n = 3$. *p value < 0.05, **p value < 0.01 were shown to be statistically significant, respectively

NPs was studied. Owing to conformational alterations in PLGA composition brought on by the acidic pH of the lysosomal compartment, DOX and MTX were released from the NPs. Figure 5 demonstrates that the amounts of DOX and MTX released at pH 5.0 were significantly ($p < 0.05$) higher than those released at pH 7.4. While the cumulative release of MTX and DOX at pH 5.0 was 81.23 ± 2.56% and 62.97 ± 2.4%, respectively, at pH 7.4, the 48-h release of MTX and DOX was 40 ± 1.69% and 38.2 ± 1.15%, respectively. Furthermore, during the first 2–4 h at pH 5.0, both medications displayed a slight burst release, which could be connected to drug surface adsorption on NPs. At pH 5.0, both drugs are released more quickly. In contrast to DOX, MTX showed a slower release kinetics. The delayed or less vigorous release of MTX may be explained by its higher interaction with PLGA and more hydrophobic nature compared to DOX [54].

Cell Uptake and its Mechanism

The cell uptake potential of both drugs was measured in MCF-7 breast cancer cell lines in order to investigate the possible capacity of DOX/MTX@PLGA NPs to internalize DOX and MTX. When NPs were incubated for 24 h instead of 4 h, as Fig. 6A illustrates, cell lines' cellular absorption of the medications increased significantly ($p < 0.05$) in comparison to free drugs.

Consequently, the cell uptake reached its maximum level after 24 h of being administered with NPs at concentrations of 2.5 µg/mL for DOX and 2.0 µg/mL for MTX, respectively. Therefore, DOX/MTX@PLGA NPs demonstrated time-dependent cellular uptake, with enhancement of 2-fold and 1.5-fold in cellular uptake relative to free DOX and MTX, respectively. The decrease in particle size and the stabilization of PLGA may have contributed to the increase in cell absorption by improving the colloidal stability of the dispersion in various dissolving media [55]. Because of their small particle size and colloidal stability, NPs are in fact more likely than free drugs to have interactions with and get absorbed by MCF-7 cancer cells.

The internalization or endocytosis of DOX/MTX@PLGA NPs was investigated in MCF-7 cancer cells. As demonstrated in Fig. 6B, nystatin administration resulted in a 58.33% decrease in DOX/MTX@PLGA NPs uptake when compared to the control group, which did not receive any inhibitors. Amiloride or chlorpromazine, however, had no effect on the internalization of NPs, indicating caveolae-mediated endocytosis. Additionally, incubation at 4 °C resulted in a 43.05% decrease in NP internalization relative to cells cultured at 37 °C, demonstrating that energy-dependent active transport is still necessary for the internalization process. Our results confirm previous research showing that NPs enter MCF-7 cells by caveolae-mediated endocytosis [56]. Additionally, using lysotracker green and either DAPI or Hoechst staining on MCF-7 cells, we assessed the intracellular distribution of DOX/MTX@PLGA NPs. Following a 12 h incubation period,

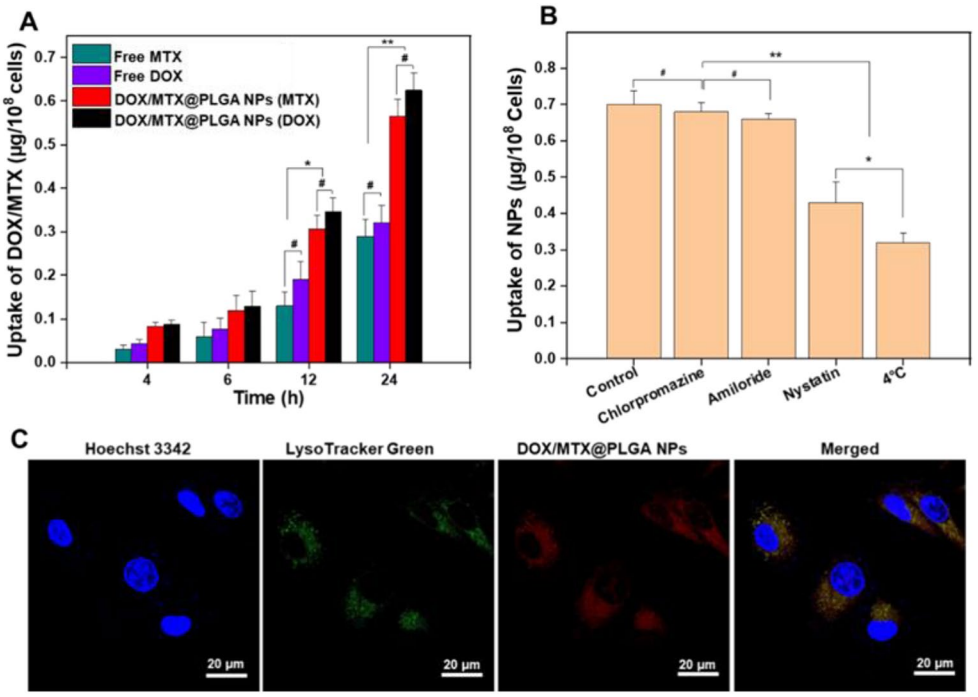

Fig. 6 (**A**) DOX/MTX@PLGA NPs cellular uptake throughout 4, 6, 12, and 24 h in relation to free DOX and MTX (2.5 μg/mL and 2.0 μg/mL), (**B**) The internalization mechanism of DOX-MTX-PLGA NPs to MCF-7 cells that have been pretreated with different inhibitors, (**C**) Intracellular distribution of DOX/MTX@PLGA NPs using confocal imaging. The data is shown as mean ± SD for $n = 3$; #p value > 0.05 and *p value < 0.05, **p value < 0.01 were shown to be statistically insignificant and significant, respectively

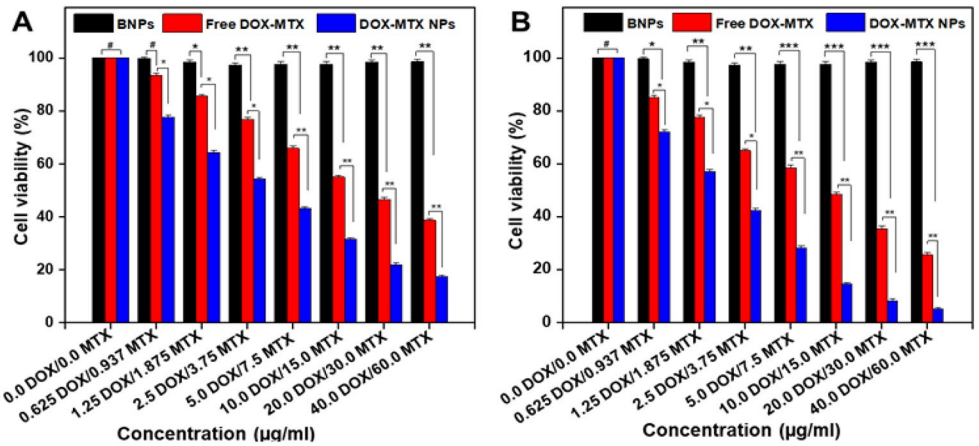

Fig. 7 MCF-7 cell viability at (**A**) 24 h. (**B**) 48 h following treatment with blank NPs, a combination of free drugs, and DOX/MTX@PLGA NPs (mean ± SD, $n = 3$), #p value > 0.05 and *p value < 0.05, **p value < 0.01, ***p value < 0.001were considered statistically insignificant and significant respectively

red-fluorescent DOX/MTX@PLGA NPs co-localized with lysosomes in 79% of cases (Fig. 6C), indicating that caveolae-mediated endocytosis is the mechanism for DOX-MTX-LGA-NP uptake into lysosomes. Our findings are consistent with previously published research that demonstrated PLGA NPs penetrate MCF-7 cells by caveolae-mediated endocytosis [57].

Cell Viability Analysis

The MTT assay was utilized to evaluate the in vitro cytotoxicity of DOX/MTX@PLGA NPs on MCF-7 cells. Following treatments with a combination of free drugs, blank, and DOX/MTX@PLGA NPs for 24 and 48 h, the growth of MCF-7 cancer cells was inhibited. Figure 7A shows that after treatment for 24 h, the development of cancer cells was likely inhibited three times by DOX/MTX@PLGA NPs in a concentration-dependent manner when compared to a free drug mixture. Furthermore, DOX/MTX@PLGA NPs dramatically decreased the viability of the cells after 48 h of treatment (Fig. 7B) when compared to the free drug mixture, suggesting that the cytotoxicity of DOX/MTX@PLGA NPs against MCF-7 cells depended on both time and concentration. Consequently, the greater cytotoxic impact of Nanoparticles may be due to the reduced particle size and higher receptor-mediated internalization of NPs by PLGA. The superior toxic effect of NPs over a combination of free drugs validated their higher absorption and internalization in cells, which is highly favorable for synergistic anti-cancer action. Furthermore, PLGA-induced hypersensitization of tumor cells could contribute to the scientific explanation of NPs' enhanced cytotoxic effect [58]. Moreover, the

MCF-7 cells treated with blank NPs exhibited the maximum levels of cell viability, demonstrating that the particles had no negative impacts on cancer cells.

Cell Apoptosis

The results of the Annexin V -APC/DAPI double labelling experiment, which was used to determine in vitro cell apoptosis, are displayed in Fig. 8. Annexin V-APC can readily pass through living cells, in contrast to DAPI, which only stains dead cells. The control group's lower left quadrant has $98.42 \pm 1.2\%$ viable cells. On the other hand, live cell percentage dropped to 76.5% and 54.61% respectively, following the treatment of free drug mixtures (DOX-MTX) and DOX/MTX@PLGA NPs. Additionally, the percentage of apoptotic cells increased to 44.88% in cells treated with DOX/MTX@PLGA NPS, compared to 23.1% in cells treated with a mixture of DOX-MTX (right upper and lower quadrant), indicating the synergistic effect of DOX/MTX@PLGA NPS against breast cancer cells [59]. The lower left quadrant shows the live cells, while right lower and right upper show the early and late apoptotic cells.

Chou Talalay Analysis

Chou Talalay analysis was used to examine the synergistic interaction between DOX and MTX in formulations of DOX-MTX-NPs [60]. Given that all NPs combinations with different DOX/MTX weight ratios outperformed both DOX and MTX NPs alone, there may be a beneficial interaction between DOX and MTX. CompuSyn utilized the Chou-Talalay technique to evaluate and measure the DOX-MTX combination's synergy [5]. Figure 9 showed the values of the combination index (CI) for the theoretical and experimental cases. The additive, antagonistic, and synergistic effects are represented by the values of $CI = 1$, > 1, and < 1, respectively. It is evident that DOX and MTX interact well in the formulations of the nanoparticles because most concentrations in all weight ratios had CI values less than 1 [61]. More importantly, a lower CI value indicates a stronger synergistic effect. [62]. The results indicated that DOX-MTX-NPs had the greatest synergistic effect at 1:1 weight ratio (CI values). Since it provided the greatest synergistic effect, the combination with a 1:1 DOX-MTX weight ratio was selected and used in later research.

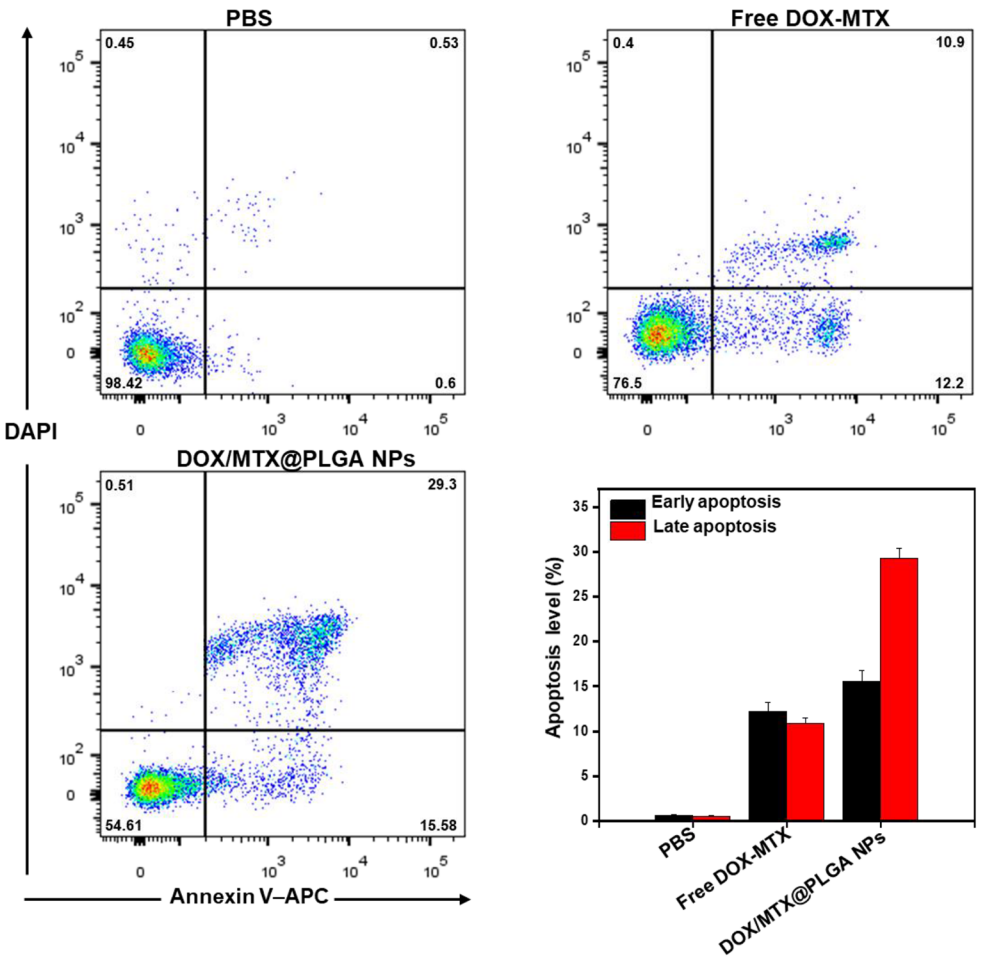

Fig. 8 Apoptosis level in MCF-7 breast cancer cells after treatment with mixture of DOX-MTX and DOX/MTX@PLGA NPs for 24 h

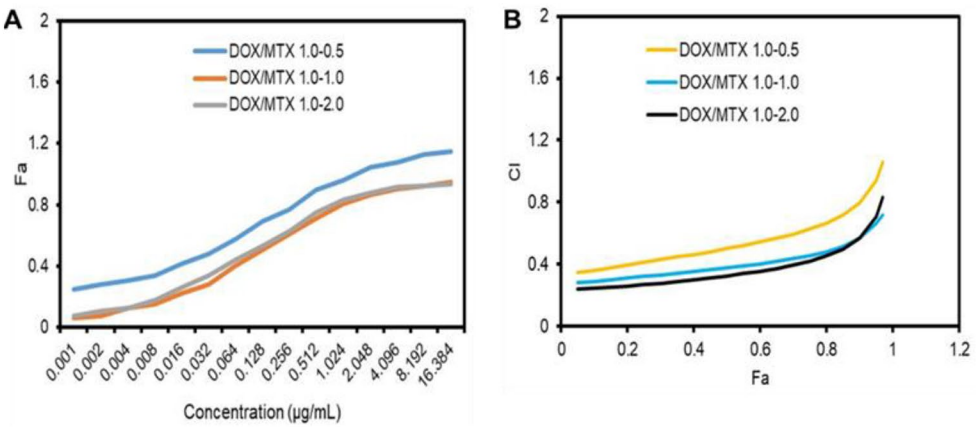

Fig. 9 (**A**) Dose response curves on MCF-7 cells treated for 48 h to weight ratios of DOX/MTX@ PLGA NPs. The percentage of affected MCF-7 cells (Fa) was shown (**B**) The combination index (CI) values for various DOX-MTX weight ratios can be identified for all Fa levels in the Chou-Talalay analysis of the dosage effect curve. The Chou-Talalay analysis model was used to determine the data, utilizing Fa levels for the actual doses

Conclusions

Polymeric nanoparticles (NPs) have had a profound and enduring impact on the field of oncology. They have produced a remarkable diversity of results in advancing drug delivery and innovative therapeutic applications from bench to bedside. They have, in fact, occasionally revealed to be more effective than liposomes and other nano carrier systems. The two anti-cancer drugs, MTX and DOX, were successfully loaded onto polymeric NPs in the present research, which allowed the drug to be transported to the tumor cell for treatment of breast cancer. Polymeric NPs demonstrated small particle size, enhanced colloidal stability, extended drug release profile, better drug loading, increased cellular uptake, and increased in-vitro cytotoxicity. Our results support the idea that, when combined and delivered via a simultaneous drug delivery system, MTX and DOX are more effective when encapsulated within polymeric NPs than when they are administered separately. Additionally, when treating breast cancer, co-loaded PLGA NPs are more successful at passively addressing the tumor. In short, our study established an appropriate platform for the synergistic delivery of combination anti-cancer drugs in the form of polymeric nanoparticles for the successful treatment of resistant breast cancer.

Acknowledgements The authors acknowledge the support from the Scientific Experiment Center, Hangzhou Institute of Medicine (HIM), Chinese Academy of Sciences.

Author Contributions Muhammad Haroon: Conceptualization, Experimental work, Investigation Methodology; Mehwish Nasim, Mohammad Y. Alfaifi, Serag Eldin I. Elbehairi, Ali A. Shati: Formal analysis, Software; Asif Nawaz: Curation, Validation: Naveed Ullah Khan, Muhammad Khurshid Alam Shah; Writing—original draft; Sheikh Abdur Rashid, Daulat Haleem Khan: Supervision, Project administration, Resources, and Visualization; Haroon Iqbal: Writing—review, editing and submission; All authors have read and agreed to the published version of the manuscript.

Funding This project received funding from Deanship of Scientific Research and Graduate Studies at King Khalid University through large Research Project under grant number R.G.P. 2/ 344/ 44.

Data Availability No datasets were generated or analysed during the current study.

Declarations

Institutional Review Board Not applicable.

Informed Consent Not applicable.

Competing Interests The authors declare no competing interests.

References

1. M. Ghazimoradi, A. Tarlani, A. Alemi, H. Hamishehkar, and M. Ghorbani: pH-responsive, magnetic-luminescent core/shell carriers for co-delivery of anticancer drugs (MTX & DOX) for breast cancer treatment, Journal of Alloys and Compounds, 2023. 936: 168257.
2. H. Sung, J. Ferlay, R.L. Siegel, M. Laversanne, I. Soerjomataram, A. Jemal, and F. Bray: Global cancer statistics 2020: GLOBOCAN estimates of incidence and mortality worldwide for 36 cancers in 185 countries, CA: a cancer journal for clinicians, 2021. 71(3): 209–249.
3. H. Iqbal, A. Razzaq, N.U. Khan, S.U. Rehman, T.J. Webster, R. Xiao, and F. Menaa: pH-responsive albumin-coated biopolymeric nanoparticles with lapatinab for targeted breast cancer therapy, Biomater Adv, 2022. 139: 213039. https://doi.org/10.1016/j.bioadv.2022.213039.
4. Y.-H. Xie, Y.-X. Chen, and J.-Y. Fang: Comprehensive review of targeted therapy for colorectal cancer, Signal transduction and targeted therapy, 2020. 5(1): 22.
5. G. Zheng, M. Zheng, B. Yang, H. Fu, and Y. Li: Improving breast cancer therapy using doxorubicin loaded solid lipid nanoparticles: Synthesis of a novel arginine-glycine-aspartic tripeptide conjugated, pH sensitive lipid and evaluation of the nanomedicine in vitro and in vivo, Biomedicine & Pharmacotherapy, 2019. 116: 109006.
6. R.S. Jadon and M. Sharma: Docetaxel-loaded lipid-polymer hybrid nanoparticles for breast cancer therapeutics, Journal of Drug Delivery Science and Technology, 2019. 51: 475–484.

7. G. Bianchini, J.M. Balko, I.A. Mayer, M.E. Sanders, and L. Gianni: Triple-negative breast cancer: challenges and opportunities of a heterogeneous disease, Nature reviews Clinical oncology, 2016. 13(11): 674–690.
8. R. Wang, L. Zhang, A. Razzaq, N.U. Khan, M.Y. Alfaifi, S.E.I. Elbehairi, A.A. Shati, H. Iqbal, and J. Ni: Albumin-coated green-synthesized zinc oxide nanoflowers inhibit skin melanoma cells growth via intra-cellular oxidative stress, International Journal of Biological Macromolecules, 2024. 263: 130694. https://doi.org/10.1016/j.ijbiomac.2024.130694.
9. Z. Fan, H. Iqbal, J. Ni, N.U. Khan, S. Irshad, A. Razzaq, M.Y. Alfaifi, S.E.I. Elbehairi, A.A. Shati, J. Zhou, and H. Cheng: Rationalized landscape on protein-based cancer nanomedicine: Recent progress and challenges, International Journal of Pharmaceutics: X, 2024. 7: 100238. https://doi.org/10.1016/j.ijpx.2024.100238.
10. S. Dash, T. Das, P. Patel, P.K. Panda, M. Suar, and S.K. Verma: Emerging trends in the nanomedicine applications of functionalized magnetic nanoparticles as novel therapies for acute and chronic diseases, Journal of nanobiotechnology, 2022. 20(1): 393.
11. H. Iqbal, F. Menaa, N.U. Khan, A. Razzaq, Z.U. Khan, K. Ullah, R. Kamal, M. Sohail, G. Thiripuranathar, B. Uzair, N.F. Rana, B.A. Khan, and B. Menaa: Two Promising Anti-Cancer Compounds, 2-Hydroxycinnaldehyde and 2- Benzoyloxycinnamaldehyde: Where do we stand?, Comb Chem High Throughput Screen, 2022. 25(5): 808–818. https://doi.org/10.2174/1386207324666210216094428.
12. Y. Wang, H. Iqbal, U. Ur-Rehman, L. Zhai, Z. Yuan, A. Razzaq, M. Lv, H. Wei, X. Ning, J. Xin, and R. Xiao: Albumin-based nanodevices for breast cancer diagnosis and therapy, Journal of Drug Delivery Science and Technology, 2023. 79: 104072. https://doi.org/10.1016/j.jddst.2022.104072.
13. J.O. Eloy, R. Petrilli, J.F. Topan, H.M.R. Antonio, J.P.A. Barcellos, D.L. Chesca, L.N. Serafini, D.G. Tiezzi, R.J. Lee, and J.M. Marchetti: Co-loaded paclitaxel/rapamycin liposomes: development, characterization and in vitro and in vivo evaluation for breast cancer therapy, Colloids and Surfaces B: Biointerfaces, 2016. 141: 74–82.
14. S.-S. Qi, J.-H. Sun, H.-H. Yu, and S.-Q. Yu: Co-delivery nanoparticles of anti-cancer drugs for improving chemotherapy efficacy, Drug delivery, 2017. 24(1): 1909–1926.
15. D. Sivadasan, M.H. Sultan, O. Madkhali, Y. Almoshari, and N. Thangavel: Polymeric lipid hybrid nanoparticles (plns) as emerging drug delivery platform—A comprehensive review of their properties, preparation methods, and therapeutic applications, Pharmaceutics, 2021. 13(8): 1291.
16. O. Maksimenko, J. Malinovskaya, E. Shipulo, N. Osipova, V. Razzhivina, D. Arantseva, O. Yarovaya, U. Mostovaya, A. Khalansky, and V. Fedoseeva: Doxorubicin-loaded PLGA nanoparticles for the chemotherapy of glioblastoma: Towards the pharmaceutical development, International journal of pharmaceutics, 2019. 572: 118733.
17. S. Karimifard, N. Rezaei, E. Jamshidifar, S. Moradi Falah Langeroodi, M. Abdihaji, A. Mansouri, M. Hosseini, N. Ahmadkhani, Z. Rahmati, and M. Heydari: pH-responsive chitosan-adorned niosome nanocarriers for co-delivery of drugs for breast cancer therapy, ACS Applied Nano Materials, 2022. 5(7): 8811–8825.
18. P. Yang, L. Zhang, T. Wang, Q. Liu, J. Wang, Y. Wang, Z. Tu, and F. Lin: Doxorubicin and edelfosine combo-loaded lipid–polymer hybrid nanoparticles for synergistic anticancer effect against drug-resistant osteosarcoma, OncoTargets and therapy, 2020: 8055–8067.
19. M. Mohajeri and A. Sahebkar: Protective effects of curcumin against doxorubicin-induced toxicity and resistance: A review, Critical reviews in oncology/hematology, 2018. 122: 30–51.
20. H. Zhang, W. Jiang, R. Liu, J. Zhang, D. Zhang, Z. Li, and Y. Luan: Rational design of metal organic framework nanocarrier-based codelivery system of doxorubicin hydrochloride/verapamil hydrochloride for overcoming multidrug resistance with efficient targeted cancer therapy, ACS applied materials & interfaces, 2017. 9(23): 19687–19697.
21. S. Rezvantalab, N.I. Drude, M.K. Moraveji, N. Güvener, Y. Shi, T. Lammers, and F. Kiessling: PLGA-based nanoparticles in cancer treatment, Frontiers in pharmacology, 2018. 9: 413087.
22. H.A. Hussein and M.A. Abdullah: Novel drug delivery systems based on silver nanoparticles, hyaluronic acid, lipid nanoparticles and liposomes for cancer treatment, Applied Nanoscience, 2022. 12(11): 3071–3096.
23. X. Yao, J. Mu, L. Zeng, J. Lin, Z. Nie, X. Jiang, and P. Huang: Stimuli-responsive cyclodextrin-based nanoplatforms for cancer treatment and theranostics, Materials Horizons, 2019. 6(5): 846–870.
24. S. Karimi and H. Namazi: Targeted co-delivery of doxorubicin and methotrexate to breast cancer cells by a pH-sensitive biocompatible polymeric system based on β-cyclodextrin crosslinked glycodendrimer with magnetic ZnO core, European Polymer Journal, 2022. 176: 111435.
25. D. Levêque, G. Becker, E. Toussaint, L.-M. Fornecker, and C. Paillard: Clinical pharmacokinetics of methotrexate in oncology, International journal of Pharmacokinetics, 2017. 2(2): 137–147.
26. V. Yang, M.J. Gouveia, J. Santos, B. Koksch, I. Amorim, F. Gärtner, and N. Vale: Breast cancer: insights in disease and influence of drug methotrexate, RSC Medicinal Chemistry, 2020. 11(6): 646–664.
27. S. Bhattacharya: Methotrexate-loaded polymeric lipid hybrid nanoparticles (PLHNPs): a reliable drug delivery system for the treatment of glioblastoma, Journal of Experimental Nanoscience, 2021. 16(1): 344–367.
28. N. Tahir, A. Madni, A. Correia, M. Rehman, V. Balasubramanian, M.M. Khan, and H.A. Santos: Lipid-polymer hybrid nanoparticles for controlled delivery of hydrophilic and lipophilic doxorubicin for breast cancer therapy, International journal of nanomedicine, 2019: 4961–4974.
29. Y. Almoshari, H. Iqbal, A. Razzaq, K. Ali Ahmad, M.K. Khan, S. Saeed Alqahtani, M.H. Sultan, and B. Ali Khan: Development of nanocubosomes co-loaded with dual anticancer agents curcumin and temozolomide for effective colon cancer therapy, Drug Delivery, 2022. 29(1): 2633–2643.
30. A. Rehman, M. Iqbal, B.A. Khan, M.K. Khan, B. Huwaimel, S. Alshehri, A.H. Alamri, R.M. Alzhrani, D.M. Bukhary, and A.Y. Safhi: Fabrication, in vitro, and in vivo assessment of eucalyptol-loaded nanoemulgel as a novel paradigm for wound healing, Pharmaceutics, 2022. 14(9): 1971.
31. A. Leonyza and S. Surini: Optimization of sodium deoxycholate-based transfersomes for percutaneous delivery of peptides and proteins, Int. J. Appl. Pharm, 2019. 11(5): 329–332.
32. F. Madani, S.S. Esnaashari, M.C. Bergonzi, T.J. Webster, H.M. Younes, M. Khosravani, and M. Adabi: Paclitaxel/methotrexate co-loaded PLGA nanoparticles in glioblastoma treatment: Formulation development and in vitro antitumor activity evaluation, Life sciences, 2020. 256: 117943.
33. M.K. Khan, B.A. Khan, B. Uzair, S. Iram Niaz, H. Khan, K.M. Hosny, and F. Menaa: RETRACTED ARTCLE: Development of Chitosan-Based Nanoemulsion Gel Containing Microbial Secondary Metabolite with Effective Antifungal Activity: In vitro and in vivo Characterizations, International Journal of Nanomedicine, 2021: 8203–8219.
34. G.R. Vaz, M.C.F. Carrasco, M.M. Batista, P.A.B. Barros, M.d.C. Oliveira, A.L. Muccillo-Baisch, V.C. Yurgel, F. Buttini, F.A.A. Soares, and L.M. Cordeiro: Curcumin and quercetin-loaded lipid nanocarriers: development of omega-3 mucoadhesive

nanoemulsions for intranasal administration, Nanomaterials, 2022. 12(7): 1073.
35. F.U. Rehman, A. Farid, S.U. Shah, M.J. Dar, A.U. Rehman, N. Ahmed, S.A. Rashid, I. Shaukat, M. Shah, and G.M. Albadrani: Self-emulsifying drug delivery systems (SEDDS): measuring energy dynamics to determine thermodynamic and kinetic stability, Pharmaceuticals, 2022. 15(9): 1064.
36. G. Babos, E. Biró, M. Meiczinger, and T. Feczkó: Dual drug delivery of sorafenib and doxorubicin from PLGA and PEG-PLGA polymeric nanoparticles, Polymers, 2018. 10(8): 895.
37. H. Tang, H. Chen, Y. Jia, X. Liu, Z. Han, A. Wang, Q. Liu, X. Li, and X. Feng: Effect of inhibitors of endocytosis and NF-kB signal pathway on folate-conjugated nanoparticle endocytosis by rat Kupffer cells, International journal of nanomedicine, 2017: 6937–6947.
38. B.R. Jermy, V. Ravinayagam, W.A. Alamoudi, D.D. Almohazey, H., L. Hussain Allehaibi, A. Baykal, and M.S.S. Toprak, T.: Targeted therapeutic effect against the breast cancer cell line MCF-7 with a CuFe(2)O(4)/silica/cisplatin nanocomposite formulation, Beilstein J Nanotechnol, 2019. 10: 2217–2228. https://doi.org/10.3762/bjnano.10.214.
39. H. Zheng, Z. Chen, A. Cai, X. Lin, X. Jiang, B. Zhou, J. Wang, Q. Yao, R. Chen, and L. Kou: Nanoparticle mediated codelivery of nifuratel and doxorubicin for synergistic anticancer therapy through STAT3 inhibition, Colloids and Surfaces B: Biointerfaces, 2020. 193: 111109.
40. Y. Choi, H.Y. Yoon, J. Kim, S. Yang, J. Lee, J.W. Choi, Y. Moon, J. Kim, S. Lim, and M.K. Shim: Doxorubicin-loaded PLGA nanoparticles for cancer therapy: molecular weight effect of PLGA in doxorubicin release for controlling immunogenic cell death, Pharmaceutics, 2020. 12(12): 1165.
41. S.A. Rashid, S. Bashir, F. Naseem, A. Farid, I.A. Rather, and K.R. Hakeem: Olive oil based methotrexate loaded topical nanoemulsion gel for the treatment of imiquimod induced psoriasis-like skin inflammation in an animal model, Biology, 2021. 10(11): 1121.
42. N.U. Khan, J. Ni, X. Ju, T. Miao, H. Chen, and L. Han: Escape from abluminal LRP1-mediated clearance for boosted nanoparticle brain delivery and brain metastasis treatment, Acta Pharmaceutica Sinica B, 2021. 11(5): 1341–1354.
43. C. Bi, X.Q. Miao, S.F. Chow, W.J. Wu, R. Yan, Y. Liao, A.H.-L. Chow, and Y. Zheng: Particle size effect of curcumin nanosuspensions on cytotoxicity, cellular internalization, in vivo pharmacokinetics and biodistribution, Nanomedicine: Nanotechnology, Biology and Medicine, 2017. 13(3): 943–953.
44. T. Sun, Y.S. Zhang, B. Pang, D.C. Hyun, M. Yang, and Y. Xia: Engineered nanoparticles for drug delivery in cancer therapy, Nanomaterials and Neoplasms, 2021: 31–142.
45. P. Liu, N. Chen, L. Yan, F. Gao, D. Ji, S. Zhang, L. Zhang, Y. Li, and Y. Xiao: Preparation, characterisation and in vitro and in vivo evaluation of CD44-targeted chondroitin sulphate-conjugated doxorubicin PLGA nanoparticles, Carbohydrate polymers, 2019. 213: 17–26.
46. S.A. Rashid, S. Bashir, H. Ullah, D.H. Khan, P.A. Shah, M.Z. Danish, M.H. Khan, S. Mahmood, M. Sohaib, and M.M. Irfan: Development, characterization and optimization of methotrexate-olive oil nano-emulsion for topical application, Pakistan Journal of Pharmaceutical Sciences, 2021. 34.
47. D. Bajas, G. Vlase, M. Mateescu, O.A. Grad, M. Bunoiu, T. Vlase, and C. Avram: Formulation and characterization of alginate-based membranes for the potential transdermal delivery of methotrexate, Polymers, 2021. 13(1): 161.
48. P. Abasian, M. Radmansouri, M.H. Jouybari, M.V. Ghasemi, A. Mohammadi, M. Irani, and F.S. Jazi: Incorporation of magnetic NaX zeolite/DOX into the PLA/chitosan nanofibers for sustained release of doxorubicin against carcinoma cells death in vitro, International journal of biological macromolecules, 2019. 121: 398–406.
49. H.R. Hussain, S. Bashir, A. Mahmood, R.M. Sarfraz, M. Kanwal, N. Ahmad, H.S. Shah, and I. Nazir: Fenugreek seed mucilage grafted poly methacrylate pH-responsive hydrogel: A promising tool to enhance the oral bioavailability of methotrexate, International Journal of Biological Macromolecules, 2022. 202: 332–344.
50. S. Gandhi and I. Roy: Doxorubicin-loaded casein nanoparticles for drug delivery: Preparation, characterization and in vitro evaluation, International journal of biological macromolecules, 2019. 121: 6–12.
51. R.M. Moshikur, M.R. Chowdhury, R. Wakabayashi, Y. Tahara, M. Moniruzzaman, and M. Goto: Ionic liquids with methotrexate moieties as a potential anticancer prodrug: Synthesis, characterization and solubility evaluation, Journal of Molecular Liquids, 2019. 278: 226–233.
52. A. Zielińska, F. Carreiró, A.M. Oliveira, A. Neves, B. Pires, D.N. Venkatesh, A. Durazzo, M. Lucarini, P. Eder, and A.M. Silva: Polymeric nanoparticles: production, characterization, toxicology and ecotoxicology, Molecules, 2020. 25(16): 3731.
53. W. Xu, Z. Li, and Y. Yin: Colloidal assembly approaches to micro/nanostructures of complex morphologies, Small, 2018. 14(35): 1801083.
54. R.M. Trujillo-Nolasco, E. Morales-Avila, B.E. Ocampo-Garcia, G. Ferro-Flores, B.V. Gibbens-Bandala, A. Escudero-Castellanos, and K. Isaac-Olive: Preparation and in vitro evaluation of radiolabeled HA-PLGA nanoparticles as novel MTX delivery system for local treatment of rheumatoid arthritis, Materials Science and Engineering: C, 2019. 103: 109766.
55. M.H. Leung and A.Q. Shen: Microfluidic assisted nanoprecipitation of PLGA nanoparticles for curcumin delivery to leukemia jurkat cells, Langmuir, 2018. 34(13): 3961–3970.
56. J. Wang, N. Li, L. Cao, C. Gao, Y. Zhang, Q. Shuai, J. Xie, K. Luo, J. Yang, and Z. Gu: DOX-loaded peptide dendritic copolymer nanoparticles for combating multidrug resistance by regulating the lysosomal pathway of apoptosis in breast cancer cells, Journal of materials chemistry B, 2020. 8(6): 1157–1170.
57. M. Tariq, M.A. Alam, A.T. Singh, Z. Iqbal, A.K. Panda, and S. Talegaonkar: Biodegradable polymeric nanoparticles for oral delivery of epirubicin: in vitro, ex vivo, and in vivo investigations, Colloids and surfaces B: biointerfaces, 2015. 128: 448–456.
58. X. Zhang, J. Liu, X. Li, F. Li, R.J. Lee, F. Sun, Y. Li, Z. Liu, and L. Teng: Trastuzumab-coated nanoparticles loaded with docetaxel for breast cancer therapy, Dose-Response, 2019. 17(3): 1559325819872583.
59. S. Javanbakht, M. Shadi, R. Mohammadian, A. Shaabani, M. Ghorbani, G. Rabiee, and M.M. Amini: Preparation of Fe3O4@SiO2@ Tannic acid double core-shell magnetic nanoparticles via the Ugi multicomponent reaction strategy as a pH-responsive co-delivery of doxorubicin and methotrexate, Materials Chemistry and Physics, 2020. 247: 122857.
60. T. Ramasamy, H. Ruttala, J.Y. Choi, T.H. Tran, J. Kim, S. Ku, H. Choi, C. Yong, and J. Kim: Engineering of a lipid-polymer nanoarchitectural platform for highly effective combination therapy of doxorubicin and irinotecan, Chemical communications, 2015. 51(26): 5758–5761.
61. M. Rahimi, K.D. Safa, and R. Salehi: Co-delivery of doxorubicin and methotrexate by dendritic chitosan-g-mPEG as a magnetic nanocarrier for multi-drug delivery in combination chemotherapy, Polymer Chemistry, 2017. 8(47): 7333–7350.
62. K.R. Roell, D.M. Reif, and A.A. Motsinger-Reif: An introduction to terminology and methodology of chemical synergy—perspectives from across disciplines, Frontiers in pharmacology, 2017. 8: 241453.